Available online at www.sciencedirect.com
ScienceDirect
Trans. Nonferrous Met. Soc. China 26(2016) 924−929
Transactions of Nonferrous Metals Society of China
www.tnmsc.cn

Effects of high temperature pre-straining on natural aging and bake hardening response of Al−Mg−Si alloys

Zhi-hong JIA, Li-peng DING, Yao-yao WENG, Zhang WEN, Qing LIU

College of Materials Science and Engineering, Chongqing University, Chongqing 400044, China

Received 4 May 2015; accepted 4 August 2015

Abstract: The influences of high temperature pre-straining (HT-PS) on the natural aging and bake hardening of Al−Mg−Si alloys were investigated by Vickers microhardness measurements, differential scanning calorimetry (DSC) analysis and transmission electron microscopy (TEM) characterization. The results show that pre-straining at 170 °C immediately after quenching can effectively resolve the rather high T4 temper hardness caused by the conventional room temperature (RT) pre-straining treatment, and give a better bake hardening response (BHR) after paint-bake cycle. HT-PS 7% at 170 °C for 10 min is chosen as the optimum process as it provides lower T4 temper hardness and better BHR. The simultaneous introduction of dislocations and Cluster (2) can significantly suppress the natural aging and promote the precipitation of β'' phase, and reduce the effects of deformation hardening by dynamic recovery.

Key words: Al−Mg−Si alloy; high temperature pre-straining; natural aging; bake hardening response

1 Introduction

Heat-treatable Al−Mg−Si alloys have been widely utilized as light-weight materials for the body panels of automobiles owing to their good age hardening [1−3]. However, the hardening response of these alloys cannot be fully exploited in the commercial paint-bake cycles due to the low temperatures and short time involved [4]. Besides, storage at room temperature (RT) before paint-bake cycle results in a low density of β'' phase (the so-called negative effect of natural aging). It is therefore essential to improve the precipitation kinetics during the paint-bake cycle and suppress the adverse effect of natural aging [5,6]. Much effort has been devoted in recent years to study the introduction of pre-aging or pre-straining shortly after quenching, which is effective in suppressing the natural aging and improving the back hardening response (BHR) of Al−Mg−Si alloys [7−10].

Pre-straining has been reported to have a substantial effect on the precipitation behavior of Al−Mg−Si alloys [11−15]. The dislocations introduced by pre-straining are believed to act as sink of quenched-in vacancies and avoid clustering at room temperature, thus suppressing the negative effect of natural aging. While during the paint-bake cycle, the dislocations could provide heterogeneous nucleation sites for the Guinier-Preston (GP) zones that easily grow and transform into β'' phase by the enhanced atomic transport [16,17]. However, the deformation hardening caused by dislocations also gives a rather high strength in T4 temper, which could harm the formability in the stamping process [8]. The unfavorable formability in T4 temper limits the application of the pre-straining treatment. In the present study, pre-straining at high temperatures (above recrystallization temperature) was employed immediately after solution heat treatment to explore whether this special process could resolve the disadvantage of RT pre-straining and maintain a good BHR after paint-bake cycle.

2 Experimental

The Al−Mg−Si alloy used in the present investigation was a typical AA6022 alloy with a composition of Al−1.11%Si−0.62%Mg−0.06%Cu−0.16%Fe−0.06%Mn (mass fraction). It was cast and homogenized at 560 °C, and hot- and cold-rolled to sheet

Foundation item: Project (2014DFA51270) supported by the International Science and Technology Cooperation Program of China; Project (51421001) supported by the Foundation for Innovative Research Groups of the National Natural Science Foundation of China
Corresponding author: Zhi-hong JIA; Tel: +86-23-65102029; E-mail: zhihongjia@cqu.edu.cn
DOI: 10.1016/S1003-6326(16)64188-2

with 1 mm in thickness. The rolled sheets were solution-treated at 560 °C for 30 min and then water-quenched to room temperature. High temperature pre-straining (HT-PS) was performed at 170 °C for 3, 5 and 10 min respectively, with different pre-strain levels (3%, 5%, 7%, 10%), and the straining was performed before the high temperature holding. For comparison, pre-straining at room temperature (RT-PS) was employed at the same pre-strain level. Several sheet samples without pre-straining (PS 0) were also prepared. All samples were then held at room temperature for 14 d. A simulated paint bake treatment referring to an artificial aging at 180 °C for 30 min was applied to the natural aged samples. A schematic representation of the heat treatment procedures is shown in Fig. 1.

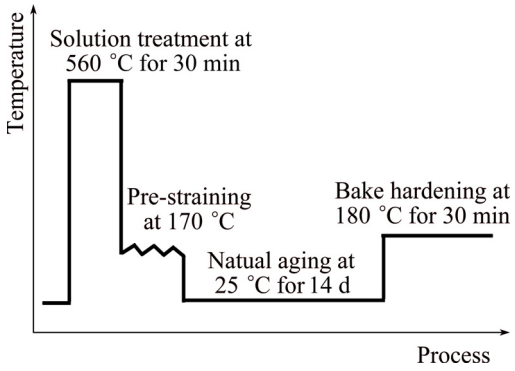

Fig. 1 Schematic representation of heat treatment procedures for AA6022 alloy

All the pre-straining treatments were performed with a tension speed of 0.3 mm/min. The hardness of samples after different heat treatments was measured using an MH−5L microhardness tester with a force of 5 N and a loading time of 10 s. Precipitation behavior was analyzed by differential scanning calorimetry (DSC) operated in an argon atmosphere using a METTLER−1100LF system ranging from 20 to 500 °C with a heating rate of 10 °C/min. Microstructure investigations were carried out on a Zeiss Libra 200FE transmission electron microscope (TEM). The specimens were prepared by electropolishing using a Struers TenuPol−5 machine. The electrolyte consisted of 30% HNO_3 in methanol and was kept at a temperature between −25 and −35 °C. For each sample, ten TEM bright-field images were taken together with the corresponding thickness measurements for the purpose of quantifying the average precipitate cross-section, length and number density. All the images were acquired along $\langle 100 \rangle_{Al}$ zone axis. A Gatan parallel electron energy loss spectrometer (EELS) was used to determine the thickness of the investigated area. A full description of the statistic methodology has been given elsewhere [18].

3 Results

The hardness curves of samples with different RT-PS treatments during 14 d RT storage and paint bake treatment are shown in Fig. 2. In the sample without pre-straining, the hardness increased from HV 56.7 to HV 84.3 during 14 d RT storage, and rose up to HV 107.4 after paint bake treatment, which was lower than that of the paint baked sample without natural aging (HV 116.3), implying that natural aging significantly increased the T4 temper hardness and reduced the BHR after paint-bake cycle, posing an unfavorable effect on formability and in-serve dent resistance. While after introducing the RT-PS treatment, the hardness of the pre-strained samples was higher than that of the un-deformed sample under each condition. With increasing the pre-straining level, both the hardness of freshly solutionized, T4 temper and paint baking samples increased gradually, as shown in Table 1. It is fair to claim that the RT-PS treatment could effectively reduce the natural aging and improve the BHR after paint bake treatment, but the over high T4 temper hardness is unfavorable to its formability.

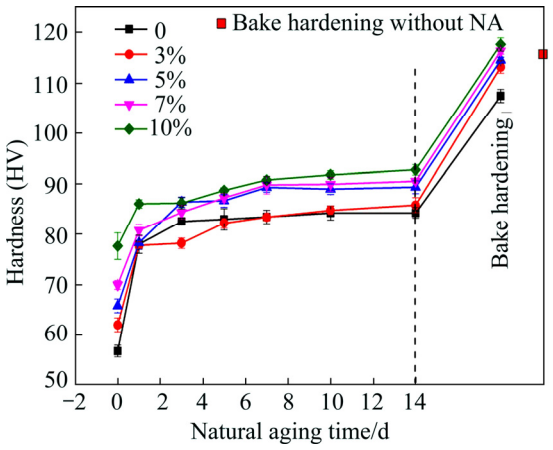

Fig. 2 Vickers hardness curves of RT-PS samples during 14 d RT storage and paint bake treatment

The hardness curves of HT-PS samples during 14 d RT storage and paint bake treatment are shown in Fig. 3. The HT-PS samples only showed a small hardness change during the RT storage and the T4 temper hardness of these samples was lower than that of the RT-PS samples, confirming that the clustering during RT storage was greatly suppressed. After paint bake treatment, nearly all the HT-PS samples showed higher BHR than those RT-PS samples at the same pre-strain level. With increasing the holding time at 170 °C, the change of natural aging hardness decreased and the BHR increased. While with the increase of HT-PS level, higher T4 temper hardness and paint baked hardness were

Table 1 T4 temper hardness, paint-baked hardness, change of natural aging hardness and BHR of RT-PS treatment and HT-PS treatment samples (HV)

Pre-strain level	RT-PS				HT-PS (10 min)			
	T4 hardness	Paint-baked hardness	Change of natural aging hardness	BHR	T4 hardness	Paint-baked hardness	Change of natural aging hardness	BHR
0	84.2	107.5	27.5	23.3				
3%	85.8	113.2	23.9	26.2	81.4	115.1	6.1	33.7
5%	89.4	114.5	23.6	25.5	79.5	115.4	2.8	35.9
7%	90.5	116.3	20.5	25.8	80.9	118.1	2.9	37.2
10%	92.8	117.5	15.2	24.8	84.2	121.3	2.1	37.1

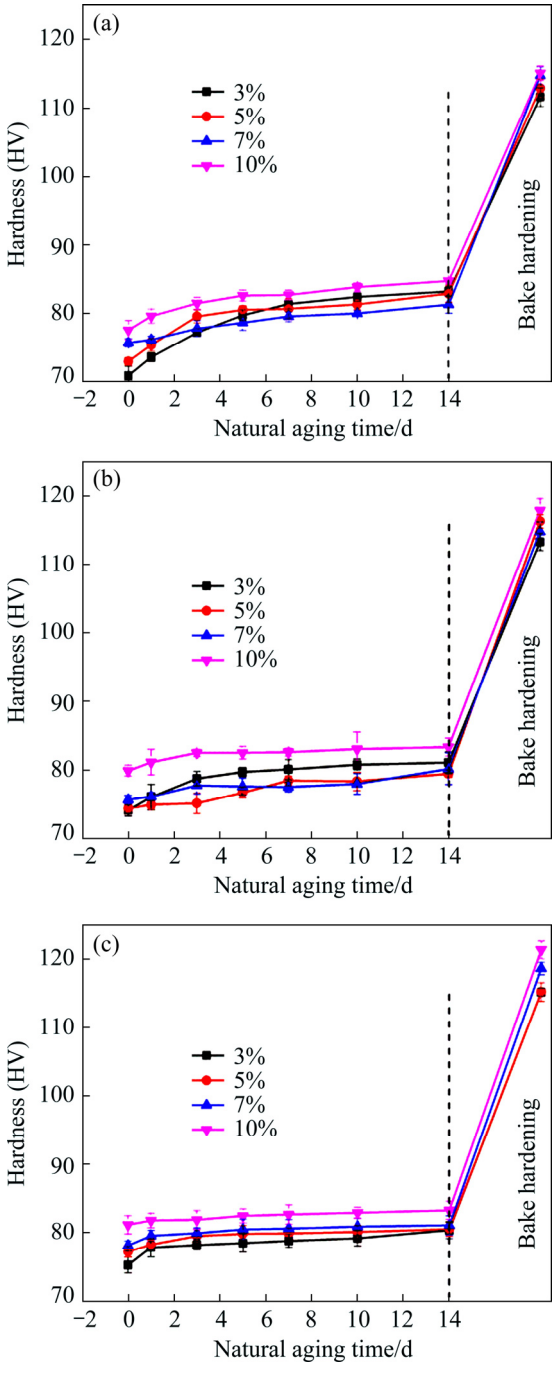

Fig. 3 Vickers hardness curves of HT-PS samples during 14 d RT storage and paint bake treatment for 3 min (a), 5 min (b) and 10 min (c)

achieved, but HT-PS 10% always resulted in higher T4 temper hardness, which is unfavorable to the alloys. Thus, HT-PS 7% for 10 min is chosen as the optimum process as it provides lower T4 temper hardness (HV 80.9) and better BHR (HV 37.2). Compared with RT-PS 7%, the T4 temper hardness of the HT-PS 7% sample decreases by about HV 9.6, and the BHR increases by about HV 12.3, as shown in Table 1, which is beneficial to the formability and in-serve dent resistance. Therefore, it can be deduced that HT-PS treatment is more effective in suppressing the natural aging and improving the BHR compared with RT-PS treatment.

In order to study the mechanism responsible for the improvement in BHR by the HT-PS treatment, DSC and TEM investigations were performed. DSC was carried out in the RT-PS 7% and HT-PS 7% (10 min) samples after 14 d RT storage and the results are shown in Fig. 4. In contract with the sample without pre-straining, both the RT-PS and HT-PS samples displayed an exothermic peak between 120 and 160 °C which links to the formation of GP zones. A dissolution trough between 180 and 220 °C, which came from the reversion of clusters during natural aging, was largely reduced or disappeared in the pre-strained samples, suggesting that both the RT-PS and HT-PS treatments could effectively suppress the natural aging [8,11].In addition, the β'' precipitation peak shifted to lower temperature for the pre-strained

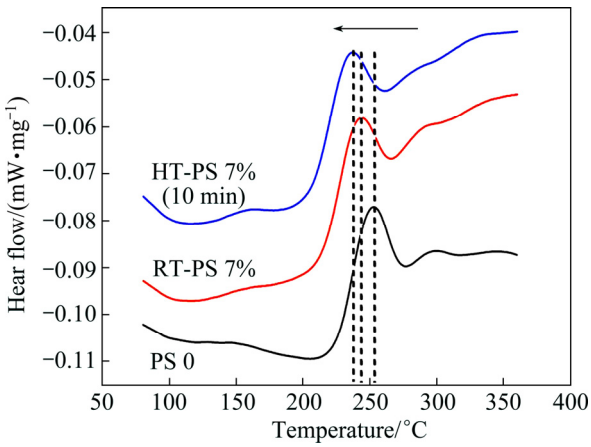

Fig. 4 DSC curves of samples under different pre-straining conditions

samples, and the HT-PS sample presented a lower β'' precipitation temperature (235.3 °C) than the RT-PS sample (242.5 °C), indicating that the HT-PS treatment is more effective in accelerating the precipitation of β'' phase.

The bright-field TEM images and corresponding selected area diffraction patterns (SADP) of the PS 0, RT-PS 7% and HT-PS 7% (10 min) samples after RT storage and paint bake treatment are shown in Fig. 5. All the images were acquired along $\langle 100\rangle_{Al}$ zone axis. In the sample without pre-straining, large numbers of dot-like precipitates were homogeneously distributed in the Al matrix, and some needle-like precipitates were also clearly observed. Most of the tiny dot-like precipitates (about 2 nm) are identified as GP zones, and some larger dot-like precipitates (3−4 nm) are the end-on sections of the β'' phase along $\langle 100\rangle_{Al}$, as evidenced by the faint rings seen in the diffraction pattern [19]. So, it can be deduced that most of GP zones in the sample without pre-straining have not evolved into the β'' phase during paint bake treatment, implying a poor BHR. While in the pre-strained samples, most of GP zones have been evolved into the β'' phase, and an inhomogeneous distribution of larger precipitates nucleated along dislocation lines was observed. The HT-PS treatment produces less dislocations than the RT-PS treatment. The microstructure quantification in Table 2 shows that the precipitates (mainly β'') in the HT-PS sample have a higher volume fraction and smaller average radius than those in the RT-PS sample, causing higher BHR, which are in agreement with the hardness measurements shown in Fig. 3.

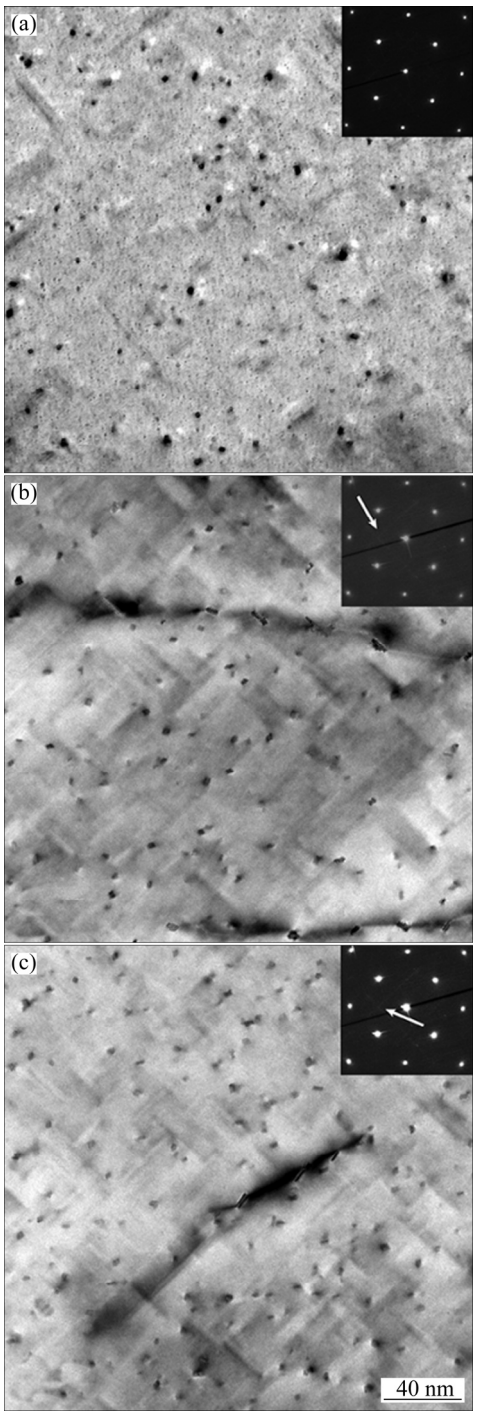

Fig. 5 Bright-field TEM images of PS 0 (a), RT-PS 7% (b) and HT-PS 7% (10 min) (c) samples after paint bake treatment (Corresponding diffraction patterns were inserted)

The HRTEM image of the precipitates along dislocation lines of the HT-PS 7% (10 min) samples after paint baking is shown in Fig. 6. From the HRTEM image and corresponding fast filtering transforms (FFT)

Table 2 Statistical distribution of precipitates in pre-aged samples after paint bake treatment

Treatment	Cross-section/nm^2	Length/nm	Number density	Volume fraction/%
RT-PS 7%	10.2±0.2	42±2.5	(1.22±0.4)×10^{-6}	0.23±0.05
HT-PS 7%	11.6±0.3	35±5.5	(1.48±0.4)×10^{-5}	0.38±0.1

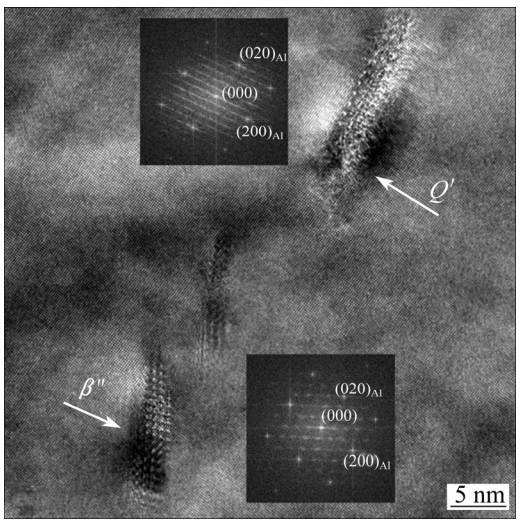

Fig. 6 HRTEM of precipitates along dislocation lines in HT-PS sample

patterns, the β'' and Q' phases can be identified [20,21]. Compared with the precipitates in the matrix, the precipitates along dislocation exhibit a coarser structure. The cross-section of β'' phase shows an elongated shape compared with a round shape β'' phase in the matrix. The precipitation of Q' phase along dislocation is due to the segregation of added trace Cu during HT-PS process. Therefore, the dislocations serve as the nucleation sites for precipitation and change the morphology, size and distribution of these precipitates, which improves the BHR of Al−Mg−Si alloys.

4 Discussion

The results presented above demonstrate that the HT-PS treatment gives better properties in T4 temper and after bake hardening compared with the RT-PS treatment. During the RT-PS treatment, dislocations introduced by the straining could act as sinks of quenched-vacancies which are essential for the clustering activities during natural aging. The relaxed supersaturation of vacancies could greatly suppress the natural aging. While during paint bake treatment, the dislocations could provide heterogeneous nucleation sites for GP zones and accelerate the precipitation of β'' phase, which is the main precipitates contributing to the peak hardness [22]. However, the dislocations also lead to deformation hardening, thus giving a rather high hardness in the T4 temper.

It is understood that the clustering of solute atoms during the pre-aging affects the precipitation of β'' phase in the final aging. SERIZAWA et al [23] reported that two types of nanoclusters, i.e., Cluster (1) and Cluster (2), were formed near room temperature and at 100 °C, respectively. The Cluster (1) structure has a wide range of Mg/Si ratio and is hardly dissolved at the paint bake temperature. The Cluster (2) has a Mg/Si ratio similar to that of the β'' phase, which enhances the formation of β'' phase during the paint bake treatment. Thus, during the HT-PS treatment, the effect of pre-straining and pre-aging simultaneously takes place. The Cluster (2) could be formed at temperatures above 100 °C, which suppresses the formation of Cluster (1) during RT storage and improves the BHR during paint bake treatment. Therefore, both the dislocations and Cluster (2) could accelerate the precipitation of β'' phase, resulting in higher BHR than of the RT-PS treatment, which are in agreement with the hardness measurements and TEM observation in Figs. 3 and 5. Besides, the deformation hardening and recovery simultaneously occur and reach a dynamic equilibrium during the HT-PS process, which reduces the effect of deformation hardening accompanying by decreased dislocation density. The remaining dislocations could still suppress the natural aging by trapping quenched-vacancies. Therefore, lower hardness of the HT-PS samples is gained in T4 temper. The HT-PS treatment resolves the detrimental effects of the RT-PS treatment, and gives a high BHR after paint-bake cycle.

5 Conclusions

1) Pre-straining immediately after quenching is effective in suppressing the natural aging and improving the BHR. The introduced dislocations can trap the quenched-vacancies and avoid clustering at RT storage, and provide heterogeneous nucleation sites for GP zones that readily grow to β'' phase during the paint-bake cycle. But a rather high T4 temper hardness due to deformation hardening is generated, which can risk the formability in the stamping process.

2) The HT-PS treatment first introduced can resolve the negative effect caused by the RT-PS treatment and give a lower T4 temper hardness and better BHR after paint-bake cycle. HT-PS 7% at 170 °C for 10 min is selected as the optimum process as it provides good properties in both T4 temper and paint-bake cycle.

3) The simultaneous occurrence of pre-straining and pre-aging promotes the precipitation of β'' phase by the introduced dislocation and Cluster (2), and the dynamic recovery process reduces the detrimental effect of deformation hardening. Therefore, the HT-PS treatment has the potential of use in industrial production.

References

[1] EDWARDS G A, STILLE K, DUNLOP G L, COUPER M J. The precipitation sequence in Al−Mg−Si alloys [J]. Acta Materialia, 1998, 46(11): 3893−3904.

[2] PEROVIC A, PEROVIC D D, WEATHERLY G C, LLOYD D J. Precipitation in aluminium alloys AA6111 and AA6016 [J]. Scripta Materialia, 1999, 41(7): 703−708.

[3] MARIOARA C D, ANDERSEN S J, RØYSET J, REISO O, GULBRANDSEN D S, NICOLAISEN T E, OPHEIM I E, HELGAKER J F, HOLMESTAD R. Improving thermal stability in Cu-containing Al−Mg−Si alloys by precipitate optimization [J]. Metallurgical and Materials Transactions A, 2014, 45(7): 2938−2949.

[4] BRYANT J D. The effects of preaging treatments on aging kinetics and mechanical properties in AA6111 aluminum autobody sheet [J]. Metallurgical and Materials Transactions A, 1999, 30(8): 1999−2006.

[5] CAO L, ROMETSCH P A, COUPER M J. Clustering behaviour in an Al−Mg−Si−Cu alloy during natural ageing and subsequent under-ageing [J]. Materials Science and Engineering A, 2013, 559: 257−261.

[6] MARTINSEN F A, EHLERS F J H, TORSAETER M, HOLMESTAD R. Reversal of the negative natural aging effect in Al−Mg−Si alloys [J]. Acta Materialia, 2012, 60(17): 6091−6101.

[7] BIROL Y, KARLIK M. Bake hardening of twin roll cast Al−Mg−Si sheet [J]. Materials Science and Technology, 2005, 21(2): 153−158.

[8] BIROL Y. Pre-straining to improve the bake hardening response of a twin-roll cast Al−Mg−Si alloy [J]. Scripta Materialia, 2005, 52(3): 169−173.

[9] DE G F, LEFEBVRE W, BLAVETTE D. 3D atom probe study of solute atoms clustering during natural ageing and pre-ageing of an Al−Mg−Si alloy [J]. Philosophical Magazine Letters, 2006, 86(4): 227−234.
[10] BIROL Y. Restoration of the bake hardening response in a naturally aged twin-roll cast AlMgSi automotive sheet [J]. Scripta Materialia, 2006, 54(12): 2003−2008.
[11] QUAINOO G K, YANACOPULOS S. The effect of cold work on the precipitation kinetics of AA6111 aluminum [J]. Journal of Materials Science, 2004, 39(15): 6495−6502.
[12] SAITO T, MURAISHI S, MARIOARA C D, ANDERSEN S J, RØYSET J, HOLMESTAD R. The effects of low Cu additions and predeformation on the precipitation in a 6060 Al−Mg−Si alloy [J]. Metallurgical and Materials Transactions A, 2013, 44(9): 4124−4135.
[13] TEICHMANN K, MARIOARA C D, ANDERSEN S J, PEDERSEN K O, GULBRANDSEN D S, KOLAR M, HOLMESTAD R, MARTHINSEN K. HRTEM study of the effect of deformation on the early precipitation behaviour in an AA6060 Al−Mg−Si alloy [J]. Philosophical Magazine, 2011, 91(28): 3744−3754.
[14] ENGLER O, SCHÄFER C, MYHR O R. Effect of natural ageing and pre-straining on strength and anisotropy in aluminium alloy AA 6016 [J]. Materials Science and Engineering A, 2015, 639: 65−74.
[15] SERIZAWA A, SATO T, MILLER M K. Effect of cold rolling on the formation and distribution of nanoclusters during pre-aging in an Al−Mg−Si alloy [J]. Materials Science and Engineering A, 2013, 561: 492−497.
[16] BIROL Y, KARLIK M. The interaction of natural ageing with straining in a twin-roll cast AlMgSi automotive sheet [J]. Scripta Materialia, 2006, 55(7): 625−628.
[17] KOLAR M, PEDERSEN K O, GULBRANDSEN-DAHL S, MARTHINSEN K. Combined effect of deformation and artificial aging on mechanical properties of Al−Mg−Si alloy [J]. Transactions of Nonferrous Metals Society of China, 2012, 22(8): 1824−1830.
[18] MARIOARA C D, ANDERSEN S J, ZANDERGEN H W, HOLMESTAD R. The influence of alloy composition on precipitates of the Al−Mg−Si system [J]. Metallurgical and Materials Transactions A, 2005, 36(3): 691−702.
[19] BIROL Y. Pre-aging to improve bake hardening in a twin-roll cast Al−Mg−Si alloy [J]. Materials Science and Engineering A, 2005, 391(1−2): 175−180.
[20] MIAO W F, LANGHLIN D E. Effects of Cu content and preaging on precipitation characteristics in aluminum alloy 6022 [J]. Metallurgical and Materials Transactions A, 1999, 31(2): 361−371.
[21] YANG W, WANG M, SHENG X, ZHANG Q, HUANG L. Precipitate characteristics and selected area diffraction patterns of the β' and Q' precipitates in Al−Mg−Si−Cu alloys [J]. Philosophical Magazine Letters, 2011, 91(2): 150−160.
[22] ANDERSEN S J, ZANDBERGEN H W, JANSEN J, TRÆHOLT C, TUNDAL U, REISO O. The crystal structure of the β'' phase in Al−Mg−Si alloys [J]. Acta Materialia, 1998, 46(9): 3283−3298.
[23] SERIZAWA A, HIROSAWA S, SATO T. Three-dimensional atom probe characterization of nanoclusters responsible for multistep aging behavior of an Al−Mg−Si alloy [J]. Metallurgical and Materials Transactions A, 2008, 39(2): 243−251.

高温预变形对 Al−Mg−Si 合金自然时效及烘烤硬化的影响

贾志宏，丁立鹏，翁瑶瑶，文 章，刘 庆

重庆大学 材料科学与工程学院，重庆 400044

摘 要：采用显微硬度测试、差示扫描量热法(DSC)和透射电镜(TEM)测试研究高温预变形工艺对 Al−Mg−Si 合金自然时效和烘烤硬化的影响。结果表明：合金固溶处理后立即进行 170 °C 预变形可以有效降低常温预变形工艺的 T4 态硬度过高等有害作用，并产生更好的烘烤硬化效果。170 °C 预变形 7%并保持 10 min 是最佳的高温预变形工艺，可以使合金获得较低的 T4 态硬度和良好的烘烤硬化效应。高温预变形过程中同时产生的位错和 Cluster(2)可以显著地抑制合金的自然时效，并促进烤漆过程中 β''相的析出，同时产生的动态回复可以有效抑制加工硬化产生的不利影响。

关键词：Al−Mg−Si 合金；高温预变形；自然时效；烘烤硬化性

(Edited by Mu-lan QIN)